


Article

Non-Uniform Turbulence Modeling in Isolated Unsteady Diffuser Computational Models for a Vaned Centrifugal Compressor

Benjamin L. Holtmann and Nicole L. Key * 

Department of Mechanical Engineering, Purdue University, West Lafayette, IN 47907, USA; bholtma@purdue.edu
* Correspondence: nkey@purdue.edu; Tel.: +1-765-494-2333

Abstract: Recent advancements in computational fluid dynamics (CFD) enable new and more complex analysis methods to be developed for early design stages. One such method is the isolated unsteady diffuser model, which seeks to reduce the computational cost of unsteady CFD when modeling diffusion systems in centrifugal compressors with vaned diffusers by isolating the diffuser from the computational domain and prescribing an unsteady and periodic inlet boundary condition. An initial iteration of this computational methodology was developed and validated for the Centrifugal Stage for Aerodynamic Research (CSTAR) at the High-Speed Compressor Laboratory at Purdue University. However, that work showed discrepancies in flow structure predictions between full-stage and isolated unsteady CFD models, and it also presented a narrow scope of only a single loading condition. Thus, this work addresses the need for improvement in the modeling fidelity. The original methodology was expanded by including a more accurate, non-uniform definition of turbulence at the diffuser inlet and modeling several loading conditions ranging from choke to surge. Results from isolated unsteady diffuser models with non-uniform turbulence modeling were compared with uniform turbulence isolated unsteady diffuser models and full-stage unsteady models at four loading conditions along a speedline. Flow structure predictions by the three methodologies were compared using 1D parameters and outlet total pressure and midspan velocity contours. The comparisons indicate a significant improvement in 1D parameter and flow structure predictions by the isolated unsteady diffuser models at all four loading conditions when including more accurate non-uniform turbulence, without a corresponding increase in computational cost. Additionally, both isolated diffuser methodologies accurately track trends in 3D flow structures along the speedline.

Keywords: centrifugal compressor; diffuser; CFD; turbomachinery



Citation: Holtmann, B.L.; Key, N.L. Non-Uniform Turbulence Modeling in Isolated Unsteady Diffuser Computational Models for a Vaned Centrifugal Compressor. *Fluids* **2024**, *9*, 270. <https://doi.org/10.3390/fluids9120270>

Academic Editors: Ernesto Benini and Francesco De Vanna

Received: 16 October 2024
Revised: 14 November 2024
Accepted: 17 November 2024
Published: 21 November 2024



Copyright: © 2024 by the authors. Licensee MDPI, Basel, Switzerland. This article is an open access article distributed under the terms and conditions of the Creative Commons Attribution (CC BY) license (<https://creativecommons.org/licenses/by/4.0/>).

1. Introduction

Recent improvements in the robustness and fidelity of computational models in turbomachinery have allowed engineers to increase the scope of their early design assessments. This is often implemented in two ways. First, increasingly complex and large models are made to simulate entire turbomachinery stages. Second, high fidelity models of individual components can be simulated with high accuracy, allowing for detailed design changes to be made early in the design process. The design of centrifugal compressors, which feature extremely complicated and unsteady flows in the impeller and vaned diffuser, has especially benefited from these improvements [1].

The flow at the outlet of an impeller in a centrifugal compressor is characterized by the jet-wake model. First hypothesized by Dean and Senoo [2], the model categorizes the impeller outlet flow into two distinct regions, the first being the jet—a region of high momentum flow adjacent to the impeller blade pressure side—and the second being the wake—a region of low momentum flow adjacent to the impeller blade suction side. The model was initially supported by circumstantial evidence from flow visualizations in

an impeller using water as the working fluid [3] and simplified component studies [4,5]. Eckardt made the first direct measurements of the jet-wake flow structure [6,7]. An example of a computed jet-wake flow structure at the outlet of a centrifugal compressor is shown in Figure 1.

When creating computational models for centrifugal compressors, considerations are made to ensure correct modelling of the impeller–diffuser interaction. This is due to the close coupling of the impeller and diffuser performance. The jet-wake flow structure exiting the impeller is the predominant driver in this interaction [8]. The impeller outlet flow, and specifically the average exit flow angle, is closely correlated with the diffuser performance [9]. Conversely, the potential field of diffuser vane leading edges imposes an unsteady condition on the impeller outlet flow, which contributes to tip leakage and potentially distinct regions of reversed flow [10]. Two different types of computational model can be used to accurately capture the impeller–diffuser interaction and pitch change. Reynolds Averaged Navier–Stokes (RANS) simulations solve for time-averaged solutions of the Navier–Stokes equations. When implementing this methodology, the interface between the rotating (impeller) and stationary (diffuser) domains is most frequently modeled using a mixing plane. This interface option for the RANS equations accounts for changes in reference frame and/or pitch [11–13]. While the performance results from this computational methodology and interface are frequently deemed “close enough” approximations, they do not accurately capture the unsteady and periodic jet-wake flow at the impeller outlet. Therefore, designers attempting to influence specific flow structures with design changes might be misled by RANS results. Unsteady RANS (URANS) simulations alleviate this issue by capturing time-varying properties in the impeller and diffuser domains. This leads to flow structure predictions that more closely resemble experimental results. However, compared to RANS, URANS simulations suffer from significantly increased computational costs. When only small design iterations are considered, these increased computational costs can be prohibitively expensive.

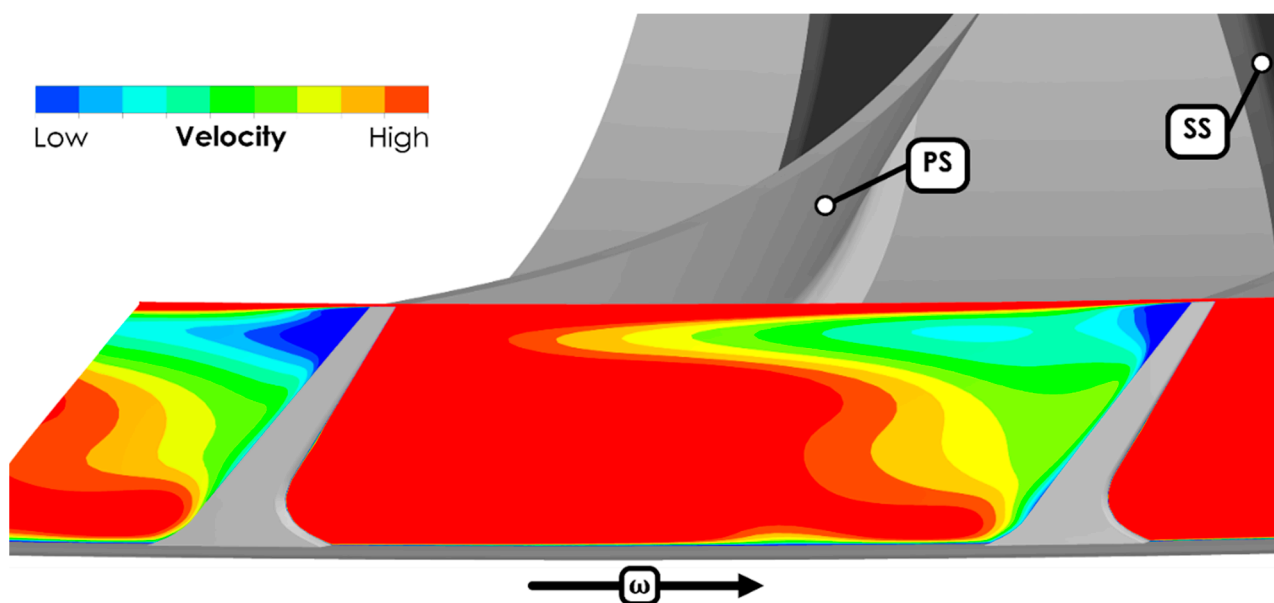


Figure 1. Jet-wake interaction at impeller outlet [1].

A method developed by Giles reduces the computational cost of URANS. The time-inclination method proposes a technique that transforms the time coordinates of the rotor and stator in the circumferential direction [14]. This allows for URANS simulations to use single passage computational domains with unequal pitches at interfaces instead of more costly full annulus simulations. Furthermore, several computational methods exist that are suited to simulating isolated blade rows. The harmonic balance method, which discretizes

the RANS equations into mathematically steady ones in which excitation frequencies appear as parameters, is suited for calculation of aerodynamic forces used in flutter and forced response simulations [15]. Isolated steady diffuser models for the vaned diffuser of a centrifugal compressor were developed by Everitt [16]. The diffuser inlet profile was taken from the impeller outlet of a single passage steady simulation using a mixing plane. The isolated steady diffuser model benefited from a reduced computational cost and was successfully applied to stall inception studies. Isolated blade row models are sensitive to the fidelity of the applied boundary condition at the inlet. An approach to modeling realistic and coherent boundary conditions at the inlet of the domain was developed by Semlitsch. This method, which is based on the method of characteristics, was successfully applied and validated at a turbine inlet [17].

These methods reduce the computational cost of URANS and provide alternatives for simulating isolated blade rows. However, in the case of the harmonic balance and isolated steady diffuser method, they neglect to transfer the periodic jet-wake flow from the impeller outlet to the diffuser inlet. Therefore, isolated unsteady diffuser models were developed for the CSTAR Gen. 1 geometry with the goal of further decreasing the computational cost of modeling time-varying flow properties in the vaned diffuser of a centrifugal compressor while also maintaining an accurate jet-wake flow structure at the diffuser inlet [1]. The challenge of applying a complex, unsteady, and periodic diffuser inlet boundary condition is further compounded by the close vicinity of the diffuser vanes to the domain inlet. An analysis which included comparing the computational results from isolated unsteady diffuser models with full-stage unsteady models and Laser Doppler Velocimetry (LDV) experimental data indicated that the isolated unsteady diffuser methodology was successful in closely matching both higher-fidelity CFD predictions and experimentally observed flow structures. However, this initial study only modeled a single geometry and loading condition (design point) [18]. The application of the methodology to a new geometry, CSTAR Gen. 2.5, is detailed in [19]. This geometry produced difficulties for the modeling approach due to the reduced vaneless space size when compared to the Gen. 1 geometry. Additionally, a detailed analysis of the flow development predicted by the full-stage and isolated models through the diffuser passage indicated a significant difference in the size and propagation of a separation region on the diffuser vane pressure side. In both models, this region originates near the shroud and diffuser vane pressure side and propagates towards the hub and passage suction side. The isolated diffuser models, described in [1,18,19], suffered from an overprediction of the size and speed of propagation of this region.

This study focuses on the improvement of the isolated unsteady diffuser computational methodology by defining a more accurate turbulence profile at the diffuser inlet. The model is then applied to four loading conditions: high loading (HL), design point (DP), low loading (LL), and near choke (NC). A comparison between the results from isolated unsteady diffuser models with and without improved turbulence modeling and full-stage unsteady models is made. A focus is placed on the modeling of the separation region in the diffuser passage by the two isolated diffuser models. However, additional 1D performance parameters are compared as well as 3D flow structures at various locations throughout the entire diffuser passage. Thereby a thorough analysis of the performance and flow structure predictions is made.

2. Experimental Facility and Methodology

The Centrifugal Stage for Aerodynamic Research (CSTAR) at the Purdue University High-Speed Compressor Laboratory was used for this work. The research facility consists of the infrastructure needed to conduct high-speed tests of a low-specific-speed centrifugal compressor and stationary diffusion system at design scale. The compression system is intended for an axi-centrifugal engine architecture [20]. As mentioned in Section 1, this study focuses on the CSTAR Gen 2.5 geometry, Figure 2. Compared to Gen. 1, this geometry included not only an additively manufactured diffuser but also a deswirl to turn the flow

back to axial. Additionally, the diffuser leading edge radius ratio was reduced from 1.08 in Gen. 1 to 1.05 in Gen. 2.5 [21].

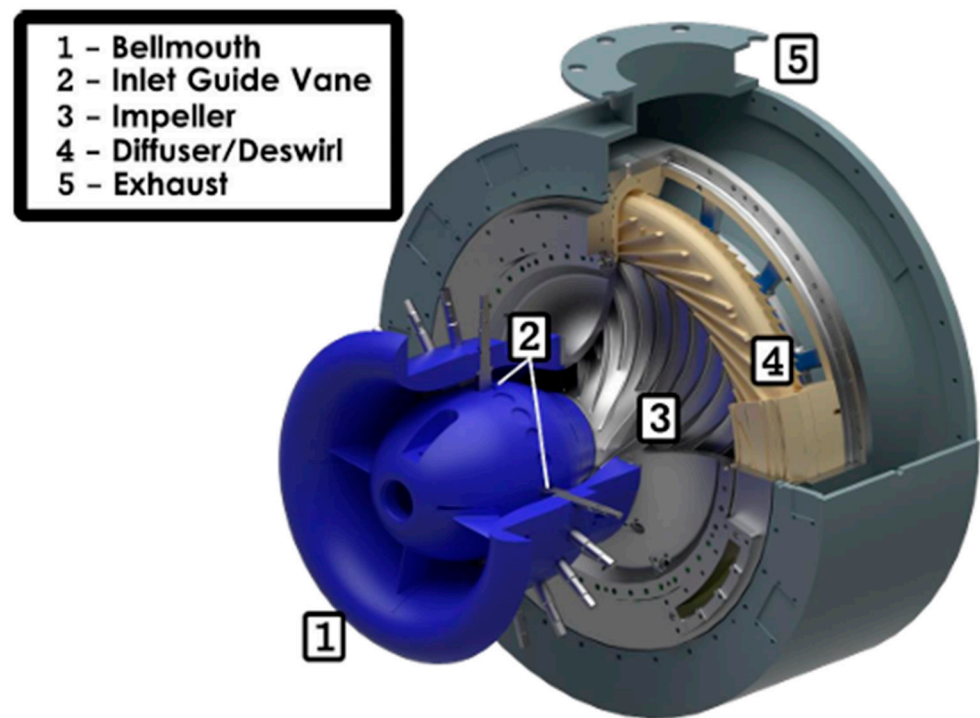


Figure 2. CSTAR Gen 2.5 compressor cutaway [22].

At the design point, which is also the best efficiency point, CSTAR Gen. 2.5 operates at about 20,800 rpm, and the total pressure ratio (TPR) is approximately 3. Inlet guide vanes are used to simulate the swirl from the latter stages of an axial compressor. The impeller consists of 15 main and 15 splitter blades, which start at 34% of the passage. Following the impeller is an additively manufactured diffusion system, with a diffuser consisting of 37 wedged vanes and a deswirl consisting of 99 vanes [23]. The facility is highly instrumented, including a significant amount of instrumentation in the diffusion system. The diffuser and deswirl include built-in static pressure taps along the vane surfaces and total pressure rakes at the vane leading edges and passage outlets. Scanivalve pressure scanning units combined with two Scanivalve rack-mounted enclosures containing DSA 3016 digital sensor arrays provide the pressure measurements. Total temperature rakes are included at the deswirl outlet. An Agilent 34980A Multifunction Switch/Measure mainframe is used to acquire temperature measurements. Combined with total pressure measurements in the facility inlet, total pressure and temperature ratio can be calculated to evaluate the performance and efficiency of the system.

The four chosen loading conditions (high loading, design point, low loading, and near choke) were defined by experimental data at 100% N_c , Figure 3. The design point loading condition was set at the best efficiency point (Figure 3b). The high loading, low loading, and near choke conditions were chosen such that trends in the flow structures could be assessed along the speedline. An additional near-surge loading condition was attempted; however, difficulties arose with the convergence of the full-stage unsteady model. Therefore, the results from that loading condition are omitted from this research.

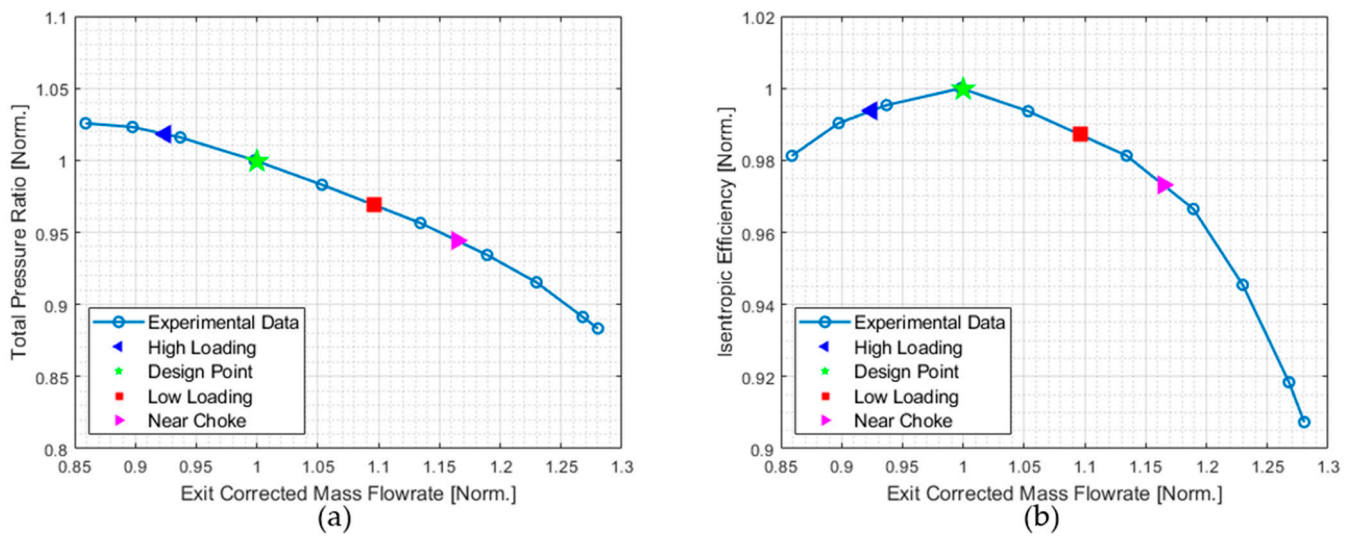


Figure 3. Compressor performance map (a) and efficiency map (b) indicating relative positions of high loading, design point, low loading, and near choke conditions.

3. Computational Methodology

The isolated unsteady diffuser computational methodology, as described in [1,18,19], is intended for diffuser design studies where only small changes in geometry are made between design iterations. These changes are unlikely to have a strong impact on the diffuser potential field, which is the primary means through which the diffuser interacts with the impeller outflow [8]. Therefore, a constant inlet profile can be used. The methodology relies on the diffuser inlet profile from a converged, full-stage, unsteady simulation. This inlet profile can then be applied, using the isolated unsteady methodology, to slightly different diffuser geometries. The best-performing diffuser design can then be assessed using higher fidelity CFD, if required. In short, the methodology makes use of the significantly reduced computational cost of isolated unsteady diffuser models to quickly iterate diffuser design in early design stages. Computational models for this study were generated in and simulated using Ansys CFX 2024 R1. Structured meshes were made for each component using Ansys TurboGrid 2024 R1, with the exception being an outlet region added to the isolated diffuser model. The outlet region, which models the curvature of the turn-to-axial and extends the computational domain to avoid reflections, is an unstructured mesh created using Ansys Meshing 2022. Outlet regions in both the full-stage and isolated models use expansion ratios such that the mesh becomes increasingly coarse towards the boundaries. The approximate element counts for both models are shown in Table 1. For the isolated diffuser model, the same diffuser domain from the full-stage model is used. The additional outlet region has an element count of approximately 3,000,000. Therefore, the isolated diffuser model has about half the element count of the full-stage model.

Table 1. Approximate element count of single passage computational domains.

Domain (Single Passage)	Approximate Element Count
Inlet Strut	1,000,000
IGV	4,000,000
Impeller	12,000,000
Diffuser (x2)	16,000,000
Deswirl	4,000,000
Total	37,000,000

The single-passage, full-stage unsteady computational domain, displayed in Figure 4a, includes the inlet, IGVs, impeller, diffuser, and deswirl. The impeller domain includes

one main blade and one splitter blade. At the inlet, ambient total pressure and total temperature at sea-level are defined. Additionally, medium intensity turbulence (5%) and an eddy viscosity ratio of 10 is assumed. An exit-corrected mass flowrate boundary condition is used at the outlet. The specific values are determined from experimental results and chosen to match the corresponding loading conditions in Figure 3. A study of computational modeling decisions applied to the CSTAR geometry by Gooding indicated the importance of modeling surface roughness [21]. Therefore, the surface roughness was defined for each computational domain based off measurements from a profilometer. A temperature profile, taken from experimental data, was defined for the impeller shroud. This temperature profile was adjusted for each loading condition. The remaining walls in the domain were modeled as adiabatic.

The Baseline Explicit Algebraic Reynolds Stress Model (BSL-EARSM) was used as the turbulence model for the full-stage and isolated diffuser models. This model was used due to a previous study in CSTAR finding that it produced the best combination of results, accuracy, and computational cost [21]. BSL-EARSM combines the baseline $k-\omega$ (turbulence kinetic energy—turbulence eddy frequency) model with the Reynolds Stress Model. This model is higher fidelity than basic, two-term models but has reduced computational costs compared to full Reynolds Stress Models. In the full-stage model, the impeller–diffuser interface is modeled using the Ansys Transient Blade Row Time Transformation (TT) model, which was originally proposed by Giles [14]. Time Transformation handles unsteady, unequal pitch problems “by transforming the time coordinates of the rotor and stator in the circumferential direction in order to make the models fully periodic in ‘transformed’ time” [24]. When using TT, Ansys recommends the pitch ratio between the domains be no more than 20%. This limit is the result of an inequality dependent on the Mach number associated with the rotor rotational speed and the Mach number associated with the circumferential velocity component [11]. Therefore, two diffuser passages were modeled. The remaining interfaces in the full-stage model feature mixing planes. A frozen rotor was used for the interface between the diffuser and the outlet in the isolated diffuser models. This method was chosen due to the pitch ratio between domains being unity. Additionally, the frozen rotor converged more quickly than a corresponding method using a mixing plane and including the deswirl [19]. Transient convergence for the full-stage and isolated models was monitored using the Clark and Grover method [25].

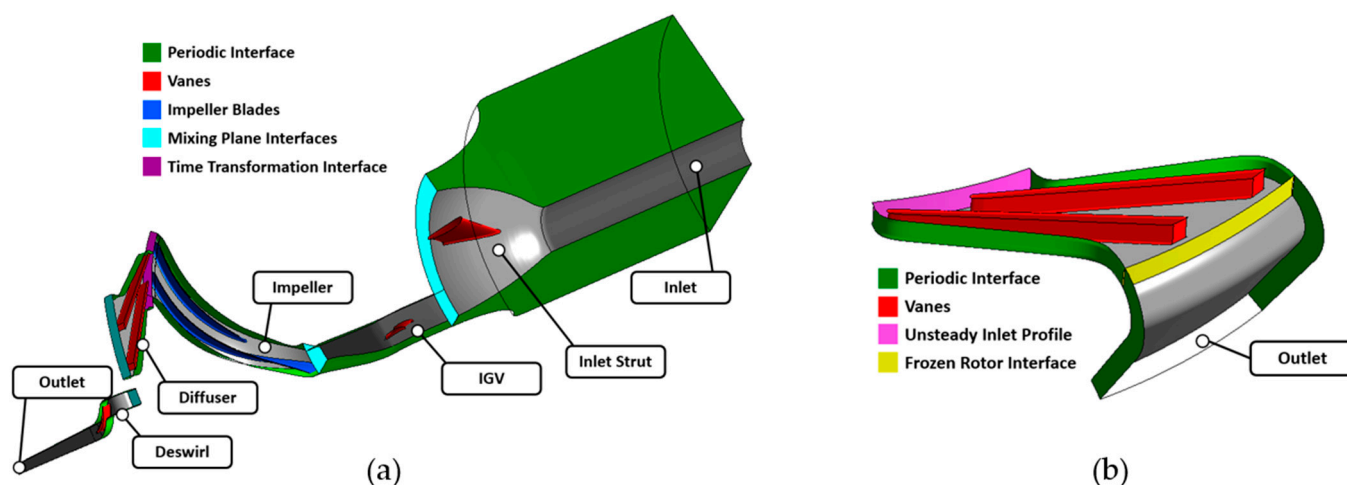


Figure 4. Definition of domains and interfaces for full-stage unsteady model (a) and isolated unsteady diffuser model (b).

Detailed descriptions of the setup of the isolated unsteady diffuser methodology are found in [1,18,19]. A short description will be provided here, with a focus placed on the differences in the methodology used for this study compared to the previous ones. Once a full-stage unsteady model is converged, the diffuser inlet profile can be extracted at each

time step across one blade passing period. For the full-stage models used in this study, one blade passing period was defined with 80 time steps, or roughly 0.3 μ s per time step. Then, using a MATLAB (R2023b) script, the individual profiles were compiled into a single unsteady and periodic profile. A detailed description of how this is achieved is found in [18]. In previous iterations of the isolated diffuser methodology, this profile consisted of five variables: total pressure, total temperature, and normalized velocity components (x , y , and z , or radial, circumferential, and axial). These variables defined the momentum, heat transfer, and velocity direction at the diffuser inlet for the isolated models. Ansys allows for Cartesian and cylindrical velocity components and spatial coordinates to be used interchangeably. For ease of visualization, cylindrical coordinates were used in this study.

To improve the modeling fidelity of isolated diffuser models, a more accurate, non-uniform, turbulence definition was given at the diffuser inlet. This was motivated by a comparison of full-stage unsteady and isolated unsteady diffuser results indicating less mixing of high momentum and low momentum flows in the isolated models. Instead of assuming medium-intensity turbulence (5%) at the diffuser inlet, turbulence kinetic energy (k) and turbulence eddy frequency (ω) were included in the unsteady periodic diffuser inlet profile. These two variables were also extracted from a full-stage, unsteady converged solution and compiled using the same methodology described in [19]. Turbulence kinetic energy and eddy frequency were chosen due to the specified turbulence model (BSL-EARSM) using them more predominantly in its calculations. It was assumed that using these variables would cause fewer issues with convergence and overconstraining of the computational domain. A summary of the components defining the isolated diffuser inlet profile, and their corresponding defining variables, is provided in Table 2.

This study includes a comparison of results from full-stage unsteady, uniform turbulence (UT) isolated unsteady diffuser, and non-uniform turbulence (NUT) isolated unsteady diffuser. Each computational methodology was evaluated at the four specified loading conditions (Figure 3). This means that this study necessitated the development and analysis of 12 computational models.

Multiple existing studies comparing computational results to experimental data in CSTAR have shown that the computational methodology previously employed produced good results and matched experimental data closely [1,22,26]. The full-stage unsteady computational methodology developed herein is heavily based on the previous existing ones. Therefore, the computational results from the isolated diffuser model presented in this paper were only compared to full-stage unsteady results, with a lesser focus placed on matching experimental data results. This is also in-line with the goal of the isolated unsteady diffuser methodology to reduce computational costs in early computational diffuser design studies.

Table 2. Summary of isolated unsteady diffuser model inlet profile definition.

Inlet Profile Component	Defined by
Momentum	Total Pressure
Heat Transfer	Total Temperature
Velocity Direction	Normalized Radial Velocity Normalized Circumferential Velocity Normalized Axial Velocity
Additionally Included for Models with Non-Uniform Turbulence	
Turbulence	Turbulence Kinetic Energy (k) Turbulence Eddy Frequency (ω)

4. Computational Results and Discussion

While matching experimental data was given less emphasis, it was still important that the full-stage unsteady results were physically representative. Figure 5 shows a comparison of the TPR and isentropic efficiency predictions by the full-stage unsteady

computational models at all four loading conditions compared to the experimental data. The computational results discussed for unsteady models presented in this section are all time-averaged. Full-stage steady state (RANS) models are included in the data set as an additional reference. These models were generated using the same computational domains as described in Section 3 for the full-stage unsteady models, with the exception being that the impeller–diffuser interface was modeled using a mixing plane instead of TT. The total pressure and total temperature ratios for the computational models were calculated using time-averaged values of total pressure and total temperature at nodes in the meshes that corresponded to the physical locations of total pressure and total temperature rake elements in the physical compressor. Both full-stage computational methodologies overpredict TPR at all four loading conditions (Figure 5a). The results from the steady and unsteady models are very similar, with the steady model having slightly more accurate TPR predictions near choke and at high loading, but the unsteady model has a more consistent TPR overprediction along the speedline. These results are reiterated in the comparison of predicted isentropic efficiencies (Figure 5b). In this case, the unsteady model produced slightly more accurate isentropic efficiency values at the design point and high loading. The overprediction of TPR and corresponding underprediction of isentropic efficiency is most likely due to an overprediction of the total temperature ratio (TTR) in the computational models. This is due to incorrect modeling of the heat transfers in the domains, as most walls are assumed to be adiabatic when, in reality, some losses due to heat transfer are expected and observed in the experimental results. A similar trend in the computational results for CSTAR Gen. 2.5 was determined by Clement [22].

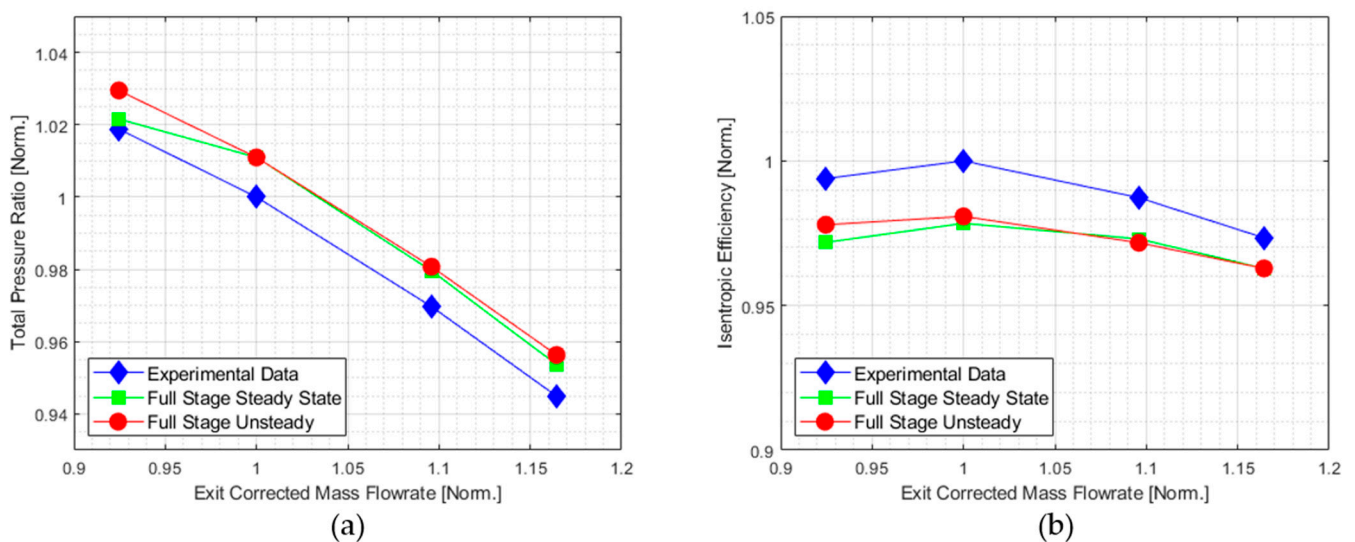


Figure 5. Comparison of total pressure ratio (a) and isentropic efficiency (b) from experimental data, full-stage steady state computational models and full-stage unsteady computational models at all four loading conditions.

The results from a comparison of 1D performance parameters typically used to judge diffuser performance are shown in Figure 6. The static pressure recovery coefficient, C_p (Figure 6a), measures the static pressure difference between the diffuser outlet and inlet, normalized by the difference in total and static pressure at the diffuser inlet. The UT and NUT isolated diffuser models underpredict static pressure recovery at all loading conditions along the speedline. The NUT isolated model is consistently closer to the value predicted by the full-stage unsteady model. This is especially true for the low loading and near choke loading conditions. The underprediction in static pressure recovery is also more consistent for the NUT isolated diffuser model. The comparison of total pressure loss shows similar trends (Figure 6b). The total pressure loss coefficient, K , measures the total pressure difference between the diffuser outlet and inlet, normalized by the difference in total and

static pressure at the diffuser inlet. Once again, the difference in the predictions by the UT and NUT isolated diffuser models are most evident at lower loading conditions. The predicted total pressure losses by the NUT isolated diffuser model are more consistent along the speedline. Both models successfully track the trend of increasing C_p and decreasing K with increasing loading.

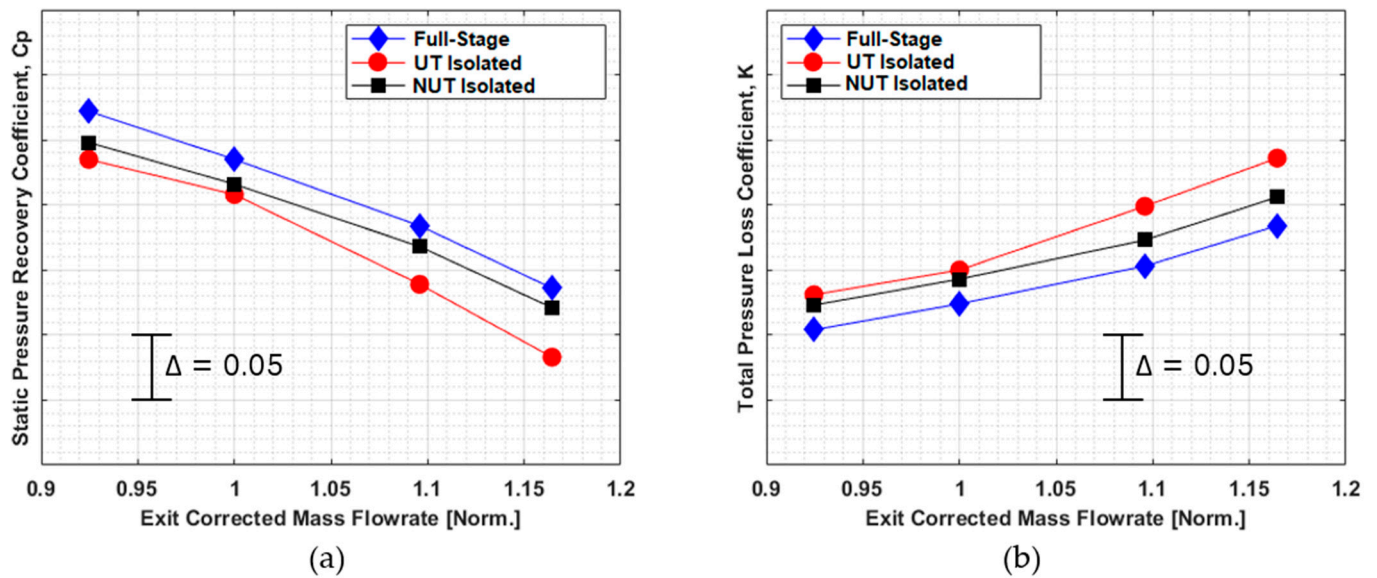


Figure 6. Comparison of static pressure recovery coefficient, C_p (a), and total pressure loss coefficient, K (b), for full-stage unsteady, UT isolated unsteady diffuser, and NUT isolated unsteady diffuser models.

The comparison of 1D performance parameters indicates that the lack of mixing of high and low momentum in the isolated unsteady diffuser models leads to lower predicted performance values. Modeling non-uniform turbulence at the diffuser inlet increases the mixing and, therefore, also increases the predicted performance. The consistent performance of the NUT isolated unsteady diffuser model along the speedline is especially important. The result is a significant improvement to the UT isolated unsteady diffuser model.

Despite the positive performance regarding predicting 1D performance parameters, it is also important that the 3D flow structure predictions by all three methodologies closely match. Therefore, several contours were generated to compare the flow structures observed at specific locations in the diffuser passage. Diffuser outlet total pressure and midspan velocity contours are compared for full-stage unsteady, UT isolated unsteady diffuser, and NUT isolated unsteady diffuser models at all four loading conditions. In these comparisons, the isolated diffuser models were analyzed with respect to their ability to predict flow structures that were consistent along the speedline.

The first flow structure comparison is made using diffuser passage outlet total pressure contours, as shown in Figure 7. The contours are generated forward looking aft, with 0% span defined as the hub and 100% span defined as the shroud. The impeller spins from low pitch (diffuser suction side) to high pitch (diffuser pressure side). The total pressure values at each loading condition are normalized by the area-averaged total pressure at the diffuser inlet for the design point loading condition. Compared to the full-stage results, both isolated models suffer from an overprediction of the separation regions on the diffuser vane suction and pressure sides at all loading conditions. The overprediction is more pronounced at lower loading conditions. The increased separation region leads to more throughflow through the core and, therefore, increased total pressure at the core. When comparing the two isolated models, it is evident that modeling non-uniform turbulence at the inlet significantly improves the flow structures. Although the separation regions are

still overpredicted, the total pressure near the endwalls is more similar to that observed in the full-stage model. Additionally, the prediction of the core location is improved. The shape of the high-momentum region in the NUT isolated diffuser model, at all loading conditions, closely resembles that of the full-stage model.

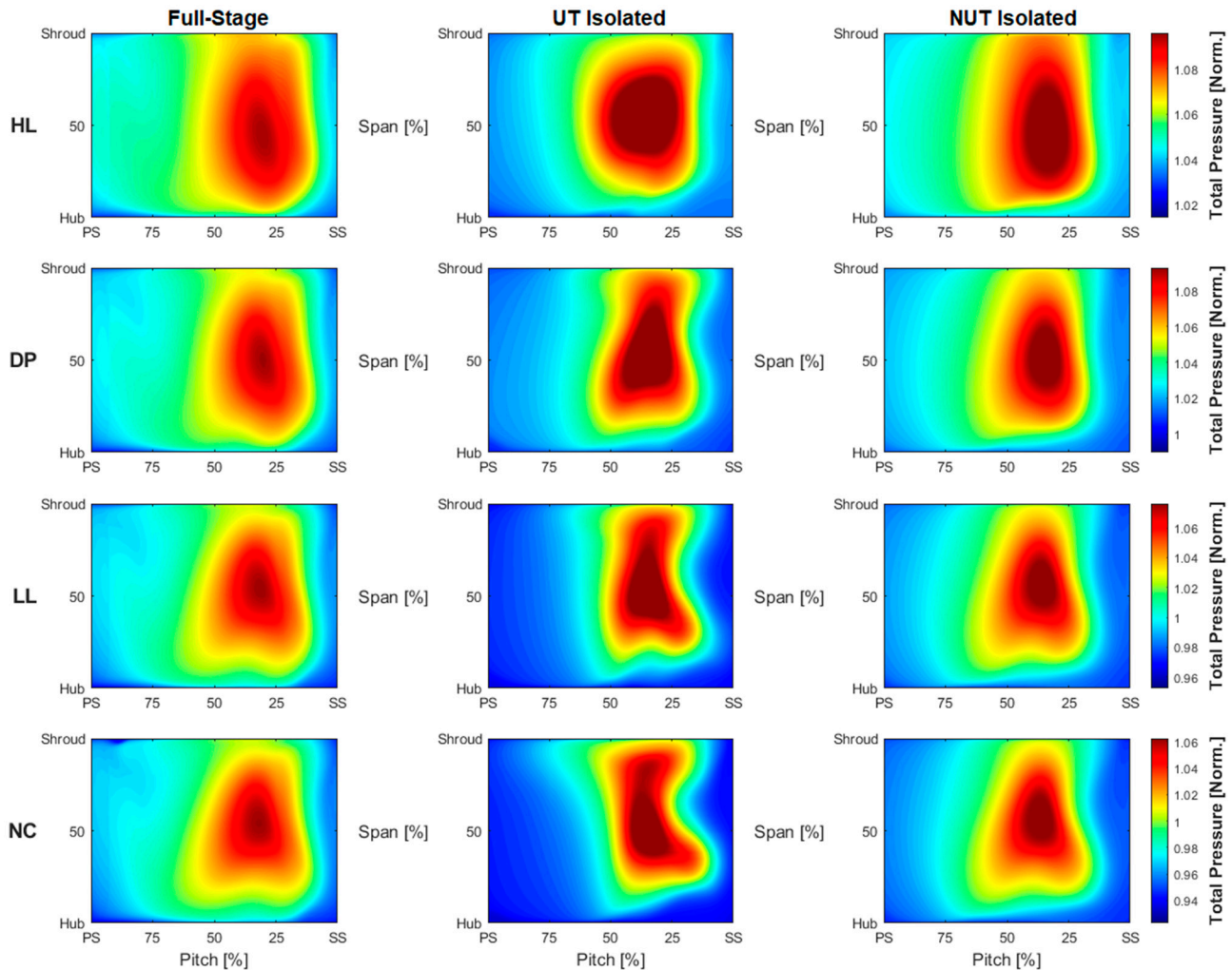


Figure 7. Diffuser passage outlet normalized total pressure contours for full-stage unsteady, UT isolated unsteady diffuser, and NUT isolated unsteady diffuser models at high loading (HL), design point (DP), low loading (LL), and near choke (NC).

To further analyze the flow structures through the diffuser passage, midspan normalized absolute velocity magnitude contours were generated for all three methodologies at all four loading conditions, Figure 8. The velocity values were normalized using the wheelspeed at 100% Nc. All contours, regardless of loading condition, predict a separation region on the diffuser vane pressure side. The size of the separation region is overpredicted by the UT isolated model. The NUT isolated model has a more accurate prediction of the size and shape of the region at all loading conditions. The contours indicated that both isolated methodologies accurately predict the velocity direction in the inlet region. This is most evident when analyzing the small shock formations and stagnation regions at the vane tip. Additionally, the isolated models indicate the same trends in separation region size and velocity magnitude as the full-stage model along the speedline.

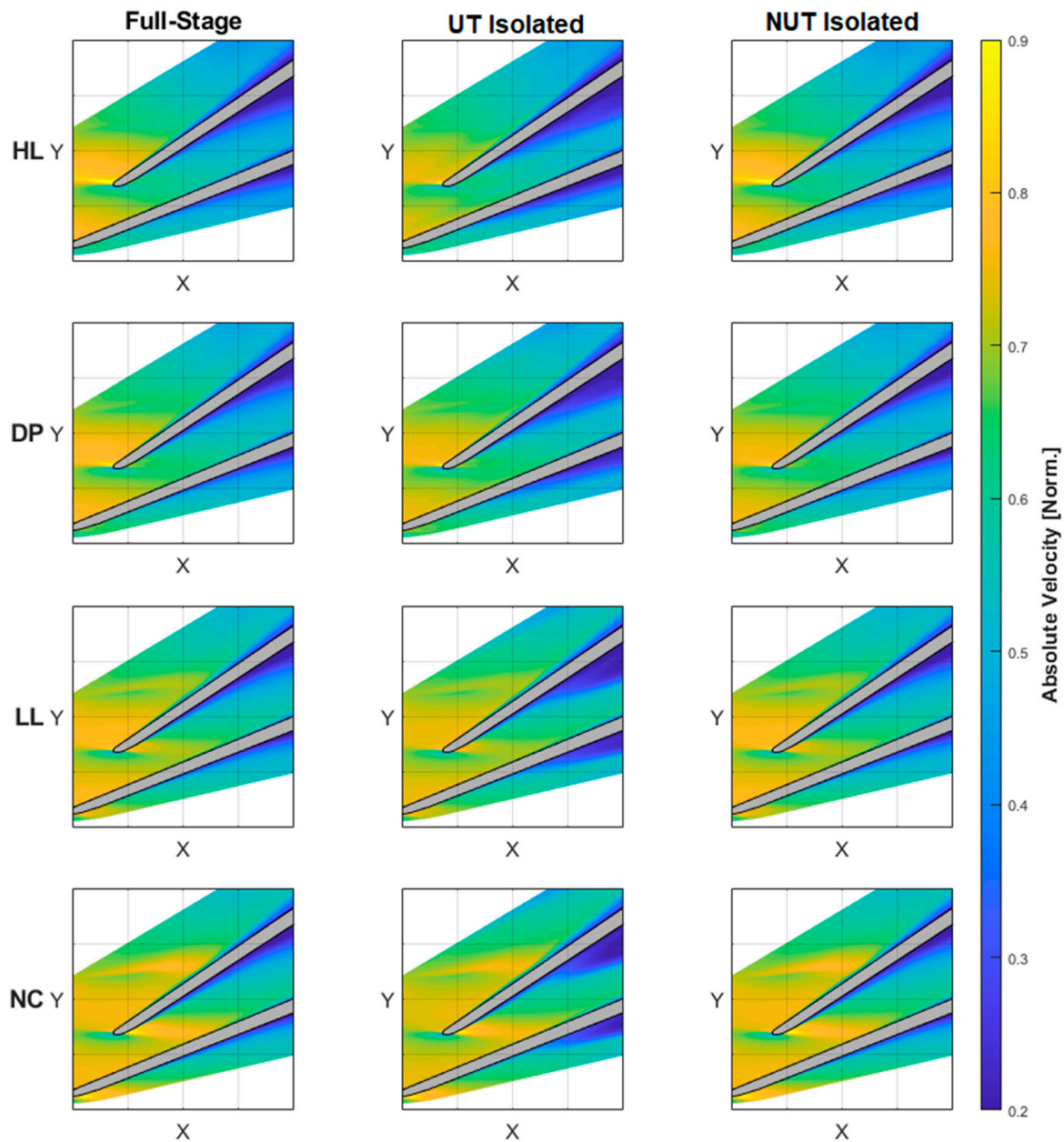


Figure 8. Normalized midspan absolute velocity magnitude contours for full-stage unsteady, UT isolated unsteady diffuser, and NUT isolated unsteady diffuser models at high loading (HL), design point (DP), low loading (LL), and near choke (NC).

The velocity predictions in the diffuser passage are further analyzed using contours indicating the difference between the full-stage and isolated models, Figure 9. In these contours, positive values indicate that the specific isolated diffuser model is overpredicting the velocity magnitude compared to the full-stage model, and negative values indicate that the specific isolated diffuser model is underpredicting the velocity magnitude compared to the full-stage model. The most obvious observation, when comparing the two isolated methodologies, is that the inclusion of non-uniform turbulence in the boundary profile significantly improved the velocity magnitude predictions throughout the entire diffuser passage. In the results from the UT isolated model, there is a small underprediction of the velocity magnitude in the inlet region. The largest differences are in the passage, where the overprediction of the size of the separation region is evident. This overprediction leads to increased velocity through the core of the passage. On the other hand, the NUT model does not suffer from these inaccuracies. The largest velocity differences are found at high loading

and appear in the diffuser inlet region and along the vane suction side. At lower loading conditions, especially the low loading and near choke conditions, velocity differences are hardly distinguishable.

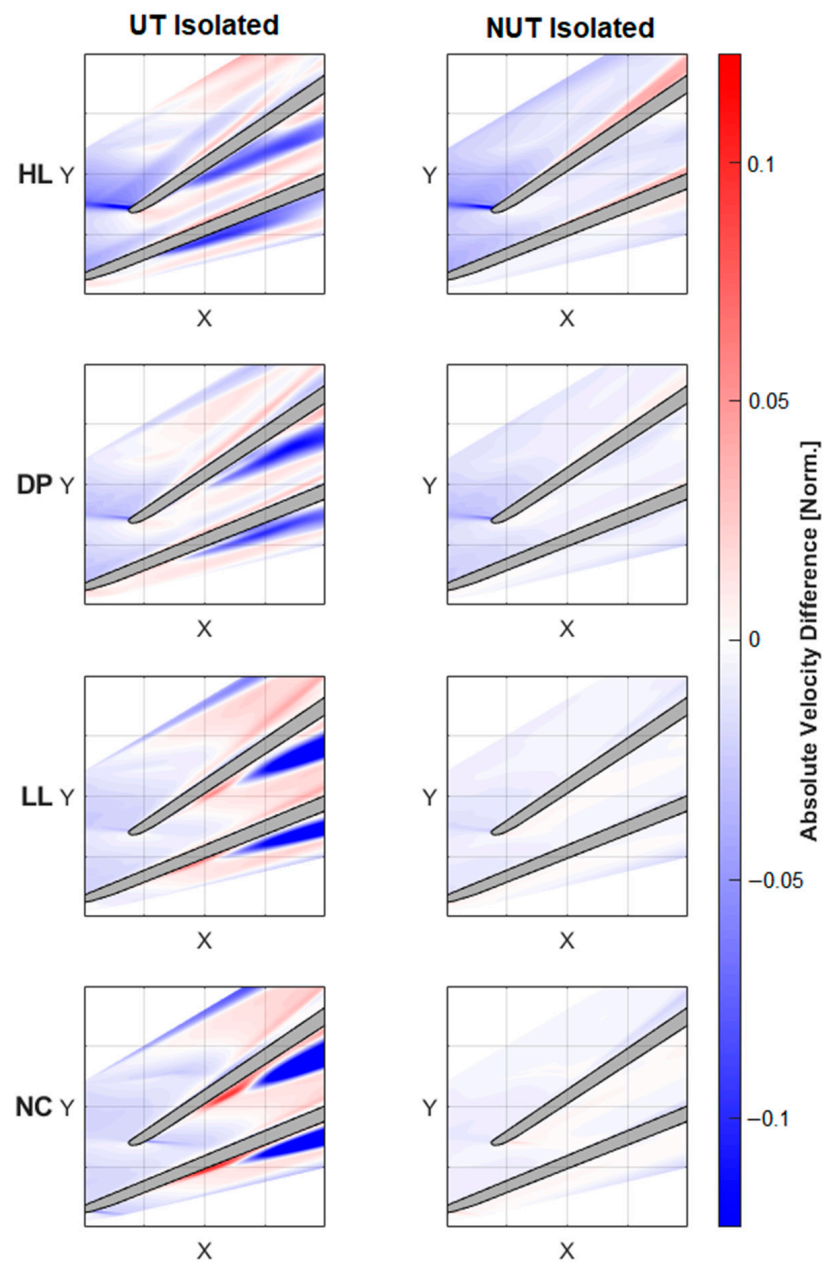


Figure 9. Difference in midspan normalized absolute velocity magnitude predictions for full-stage unsteady, UT isolated unsteady diffuser, and NUT isolated unsteady diffuser models at high loading (HL), design point (DP), low loading (LL), and near choke (NC).

When analyzing the flow structure predictions by the UT and NUT isolated unsteady diffuser models, the ability to track trends along the speedline was considered. The results from Figures 7–9 indicate that both isolated models are successfully able to do this. The trends in size of the separation region in the diffuser passage and magnitude of total pressure and velocity throughout the passage are correctly tracked along the speedline. The benefit of including non-uniform turbulence in the inlet condition comes in the accuracy of the flow structure predictions. The NUT isolated unsteady diffuser model consistently produces more accurate flow structure predictions when compared to the UT isolated unsteady diffuser model and the full-stage results. However, the UT isolated model is also

able to successfully capture trends in the full-stage unsteady model along the speedline. Therefore, when using the isolated unsteady diffuser methodology to accurately model trends along a speedline, non-uniform turbulence modeling is not a must.

At the design point loading condition, total pressure differences between the full-stage model and the two isolated diffuser models at the diffuser throat, 50% chord, and passage outlet are compared, as shown in Figure 10. Again, positive values indicate an overprediction of total pressure by the isolated model compared to the full-stage results, and negative values indicate an underprediction. The modeling fidelity benefit of including non-uniform turbulence is already evident at the throat. The UT isolated unsteady diffuser model is plagued by a significant underprediction of total pressure near the endwalls, especially near the pressure-side hub. This misrepresentation of the flow at the throat is significantly reduced when including non-uniform turbulence in the inlet profile. Additionally, as the flow progresses through the diffuser passage, the magnitude differences in total pressure in the NUT isolated unsteady diffuser model decrease. At the 50% chord location, a more significant underprediction of total pressure is captured by the UT isolated diffuser model between 50% and 75% pitch and around 25% span. At this location, the separation region predicted by the model near the vane pressure side and hub at the throat migrates spanwise downwards towards the core of the flow. This then causes the increased total pressure observed near the vane suction side. This flow pattern is not observed in the NUT model. Instead, at the 50% chord location, only small differences in total pressure exist throughout the contour. A pattern in the differences was not distinguishable at this location. The results at the passage outlet reiterate those in Figure 7. Decreased total pressure is observed near the endwalls for both isolated models, and this, in turn, leads to increased total pressure through the core. The magnitude differences in the NUT isolated model are lower than in the UT model.

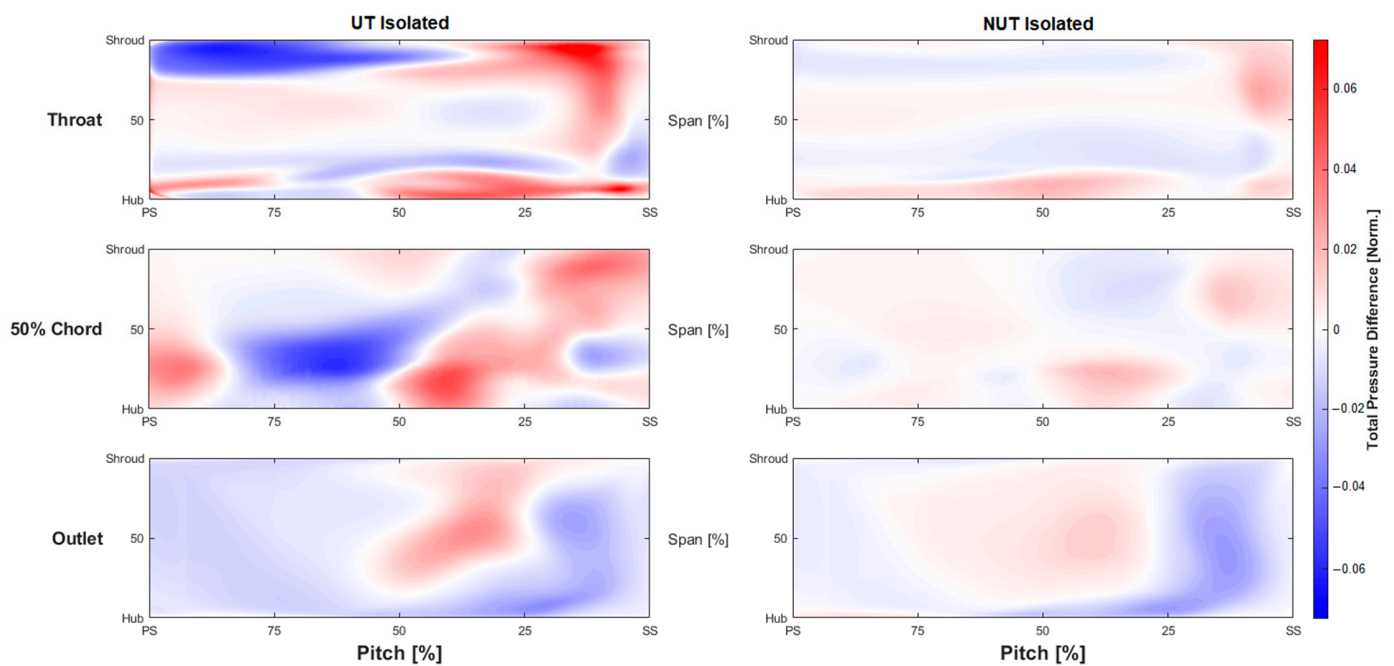


Figure 10. Normalized total pressure differences at diffuser throat, 50% chord, and diffuser passage outlet at design point loading for UT isolated unsteady diffuser and NUT isolated unsteady diffuser models.

Lastly, the computational cost to solve was quantified as the product of the time until a converged solution was reached, CPUs used, and element count in the solved mesh for each of the computational methodologies at the design point loading condition. The numerical results are summarized in Table 3. Both isolated models are computationally much less costly than the full-stage unsteady model. Including non-uniform turbulence

in the isolated diffuser methodology only slightly increased the computational cost. The trends observed in Table 3 were true when conducting the same analysis for all four loading conditions along the speedline.

Table 3. Computational cost to solve for UT isolated diffuser, NUT isolated diffuser, and full-stage models at the design point loading condition.

	Cost to Solve [Time × CPUs × Element Count]	Normalized Cost to Solve
UT Isolated	8.26×10^{14}	14.2%
NUT Isolated	8.35×10^{14}	14.3%
Full Stage	5.84×10^{15}	100%

5. Conclusions

The goals of this study were twofold; first, to increase the fidelity of isolated unsteady diffuser modeling by including non-uniform turbulence kinetic energy and turbulence eddy frequency in the diffuser inlet profile. Secondly, the goal was to apply the isolated unsteady diffuser computational methodology with non-uniform inlet turbulence quantities to multiple loading conditions along the speedline. A focus was placed on the ability of the isolated unsteady diffuser models to track trends along the speedline and accurately predict 3D flow structures at each loading condition.

Both UT and NUT isolated diffuser models were successful in tracking trends of 1D performance parameters along the speedline. Including non-uniform turbulence in the diffuser inlet profile improved the predictions at all loading conditions, especially at the low loading and near choke conditions. Diffuser outlet total pressure and midspan velocity contours indicate that the UT isolated diffuser model captured the 3D flow structure trends from the full-stage unsteady model along the speedline. However, there are notable differences in the structures. These were most significant regarding the prediction the separation regions along the diffuser vane pressure and suction sides. The overprediction of these separation regions resulted in increased total pressure and velocity magnitude through the core. When non-uniform turbulence is included in the isolated diffuser model, these differences are reduced. While a small overprediction of the total pressure through the core still exists, the size of the separation regions is significantly more accurate when compared to the full-stage model. The magnitude of the velocity differences at midspan are also more accurate.

Overall, the inclusion of non-uniform turbulence modeling at the diffuser inlet significantly improved the performance and flow structure predictions. Since these improvements are only associated with a minor increase in computational cost, it is recommended that future implementations of the isolated unsteady diffuser computational methodology include higher fidelity non-uniform turbulence modeling. The chosen turbulence variables of turbulence kinetic energy and turbulence eddy frequency can be varied depending on the chosen turbulence model.

The results from this study, and previous ones [1,18,19], indicate that isolated unsteady diffuser models are able to accurately capture 3D flow structures at multiple loading conditions closer to choke and surge and track trends along speedlines. Future improvements should focus on the implementation of the methodology in diffuser design studies and determination of when the coupling between the impeller and diffuser is affected such that the constant inlet profile assumption with changing diffuser geometries cannot be utilized.

Author Contributions: Conceptualization, B.L.H.; Methodology, B.L.H.; Validation, B.L.H.; Formal analysis, B.L.H.; Writing—original draft, B.L.H.; Writing—review & editing, N.L.K.; Supervision, N.L.K.; Project administration, N.L.K. All authors have read and agreed to the published version of the manuscript.

Funding: This research received no external funding.

Data Availability Statement: The datasets presented in this article are not readily available because the data are part of an ongoing study. Requests to access the datasets should be directed to Nicole Key (nkey@purdue.edu).

Acknowledgments: The authors are grateful to Rolls-Royce for allowing the use of the rig geometry and the experimental data for validating this computational study.

Conflicts of Interest: The authors declare no conflicts of interest.

References

1. Shapochka, M.Y. Stability Enhancement in Aeroengine Centrifugal Compressors Using Diffuser Recirculation Channels. Master's Thesis, Purdue University, West Lafayette, IN, USA, 2022.
2. Dean, R.C.; Senoo, Y. Rotating Wakes in Vaneless Diffusers. *J. Basic Eng.* **1960**, *82*, 563–570. [[CrossRef](#)]
3. Fischer, K.; Thoma, D. Investigation of the Flow Conditions in a Centrifugal Pump. *J. Fluids Eng.* **1932**, *54*, 141–154. [[CrossRef](#)]
4. Moore, J. A Wake and an Eddy in a Rotating, Radial-Flow Passage—Part 1: Experimental Observations. *J. Eng. Power* **1973**, *95*, 205–212. [[CrossRef](#)]
5. Moore, J. A Wake and an Eddy in a Rotating, Radial-Flow Passage—Part 2: Flow Model. *J. Eng. Power* **1973**, *95*, 213–219. [[CrossRef](#)]
6. Eckardt, D. Detailed Flow Investigations Within a High-Speed Centrifugal Compressor Impeller. *J. Fluids Eng.* **1976**, *98*, 390–399. [[CrossRef](#)]
7. Eckardt, D. Investigation of the Jet-Wake Flow of a Highly-Loaded Centrifugal Compressor Impeller; NASA, TM-75232. 1978. Available online: <https://ntrs.nasa.gov/citations/19780008108> (accessed on 24 July 2024).
8. Ziegler, K.U.; Gallus, H.E.; Niehuis, R. A Study on Impeller-Diffuser Interaction—Part I: Influence on the Performance. *J. Turbomach.* **2003**, *125*, 173–182. [[CrossRef](#)]
9. Everitt, J.N.; Spakovszky, Z.S.; Rusch, D.; Schiffmann, J. The Role of Impeller Outflow Conditions on the Performance of Vaned Diffusers. *J. Turbomach.* **2017**, *139*, 041004. [[CrossRef](#)]
10. Shum, Y.K.P.; Tan, C.S.; Cumpsty, N.A. Impeller-Diffuser Interaction in a Centrifugal Compressor. *J. Turbomach.* **2000**, *122*, 777–786. [[CrossRef](#)]
11. ANSYS. *CFX-Solver Modeling Guide*, 1st ed.; ANSYS: Canonsburg, PA, USA, 2017; Volume 18.
12. Dawes, W.N. A Simulation of the Unsteady Interaction of a Centrifugal Impeller With Its Vaned Diffuser: Flow Analysis. *J. Turbomach.* **1995**, *117*, 213–222. [[CrossRef](#)]
13. Denton, J.D. The Calculation of Three-Dimensional Viscous Flow Through Multistage Turbomachines. *J. Turbomach.* **1992**, *114*, 18–26. [[CrossRef](#)]
14. Giles, M.B. Calculation of Unsteady Wake/Rotor Interaction. *J. Propuls.* **1987**, *4*, 356–362. [[CrossRef](#)]
15. Ekici, K.; Hall, C. Nonlinear Analysis of Unsteady Flows in Multistage Turbomachines Using Harmonic Balance. *AIAA J.* **2007**, *45*, 1047–1057. [[CrossRef](#)]
16. Everitt, J.N.; Spakovszky, Z.S. An Investigation of Stall Inception in Centrifugal Compressor Vaned Diffuser. *J. Turbomach.* **2013**, *135*, 011025. [[CrossRef](#)]
17. Semlitsch, B. Imposing Realistic Unsteady Flow Structures Through Inflow Boundary Conditions. In Proceedings of the 30th AIAA/CEAS Aeroacoustics Conference, Rome, Italy, 4–7 June 2024. [[CrossRef](#)]
18. Holtmann, B.; Shapochka, M.; Key, N. Development and Validation of an Isolated Unsteady Diffuser Computational Model for a Vaned Centrifugal Compressor. In Proceedings of the ASME Turbo Expo, London, UK, 24–28 June 2024. [[CrossRef](#)]
19. Holtmann, B. Expanding the Scope of Isolated Unsteady Diffuser Computational Modeling. Master's Thesis, Purdue University, West Lafayette, IN, USA, 2024.
20. Methel, J.; Gooding, W.J.; Fabian, J.C.; Key, N.L.; Whitlock, M. The Development of a Low Specific Speed Centrifugal Compressor Research Facility. In *ASME Turbo Expo 2016: Turbomachinery Technical Conference and Exposition, Volume 2D: Turbomachinery*, Seoul, Republic of Korea, 13–17 June 2016; American Society of Mechanical Engineers: New York, NY, USA, 2016. [[CrossRef](#)]
21. Gooding, W.J.; Meier, M.A.; Key, N.L. The Impact of Various Modeling Decisions on Flow Field Predictions in a Centrifugal Compressor. *J. Turbomach.* **2021**, *143*, 101006. [[CrossRef](#)]
22. Clement, J.T. Experimental and Numerical Evaluation of Stationary Diffusion System Aerodynamics in Aeroengine Centrifugal Compressors. Master's Thesis, Purdue University, West Lafayette, IN, USA, 2024.
23. Clement, J.T.; Coon, A.T.; Key, N.L. Development of an Additively Manufactured Stationary Diffusion System for a Research Aeroengine Centrifugal Compressor. *J. Turbomach.* **2025**, *147*, 031004. [[CrossRef](#)]
24. ANSYS. *CFX-Solver Theory Guide*, 1st ed.; ANSYS: Canonsburg, PA, USA, 2016; Volume 17.

-
25. Clark, J.P.; Grover, E.A. Assessing Convergence in Predictions of Periodic-Unsteady Flowfields. *J. Turbomach.* **2006**, *129*, 740–749. [[CrossRef](#)]
 26. Coon, A.T. Utilization of Additive Manufacturing in the Development of Stationary Diffusion Systems for Aeroengine Centrifugal Compressors. Master's Thesis, Purdue University, West Lafayette, IN, USA, 2023.

Disclaimer/Publisher's Note: The statements, opinions and data contained in all publications are solely those of the individual author(s) and contributor(s) and not of MDPI and/or the editor(s). MDPI and/or the editor(s) disclaim responsibility for any injury to people or property resulting from any ideas, methods, instructions or products referred to in the content.